In situ gelatinase-responsive and thermosensitive nanocomplex for local therapy of gastric cancer with peritoneal metastasis

Xinyue Wang [a,1], Jiahui Gao [b,1], Chunhua Li [c,1], Chen Xu [c], Xiang Li [a], Fanyan Meng [a], Qin Liu [a], Qin Wang [a], Lixia Yu [a], Baorui Liu [a,**], Rutian Li [a,*]

[a] The Comprehensive Cancer Centre of Nanjing Drum Tower Hospital, The Affiliated Hospital of Nanjing University Medical School & Clinical Cancer Institute of Nanjing University, Nanjing, China
[b] Suzhou Yongding Hospital, Suzhou, China
[c] Nanjing Drum Tower Hospital, Clinical College of Traditional Chinese and Western Medicine, Nanjing University of Chinese Medicine, China

ARTICLE INFO

ABSTRACT

Intraperitoneal chemotherapy (IPC) has been considered as an effective therapy for advanced gastric cancer (GC) especially those with peritoneal metastasis, while limited effectiveness, complications caused by chemotherapeutics and repeated infusion procedures restrict the application of IPC. In this study, to enhance the efficacy and safety of IPC, we intended to establish a biocompatible and biodegradable nanocomplex composed of intelligent gelatinase-responsive nanoparticles (NPs) and thermosensitive gel, which were prepared from different compositions of poly (ethyleneglycol)–poly (3-caprolactone) (PEG–PCL). Cancer stem cells (CSCs) inhibitor Salinomycin (SAL) and non-CSC inhibitor Docetaxel (DOC) were co-loaded in the NPs and delivered by liquid PEG-PCL-PEG gel (PECE) at room temperature, which was able to target tumor and formed a gel in situ at body temperature. Compared with free SAL-DOC solution administered at the same dose, PECE NP group inhibited intraperitoneal disseminated gastric cancer growth more remarkably, some of which even achieved complete response (CR) and continued for more than 2 weeks. Cytometric analysis of cellular suspension from abdominal tumor tissues showed that the proportion of CSCs (CD44+CD133+) and the expression of PD-L1 on the tumor cells in the PECE NP group were the lowest. In the allograft mouse models of GC, PECE NP significantly improved the infiltration of M1 macrophages into the tumor bed in vivo. This design may provide biodegradable smart drug-delivery system for potential application in IPC.

1.Introduction

Gastric cancer (GC) is the second leading cause of cancer death globally [1]. Unlike other prevalent malignancies, GC is considered as a locoregional more than a systemic disease [2–4]. Peritoneal metastasis is one of the most important prognostic factors in gastric cancer patients, which is the first/sole site of tumor recurrence after D2 gastrectomy in 12%–40% of patients [5]. Gastric carcinoma patients with peritoneal carcinomatosis have shown poor survival rate and short survival time, ranging from 8 to 13 months [6]. Although systemic chemotherapy can marginally improve the survival after curative surgery in GC, long-term control of distant metastasis is rarely achieved [7].

With the urgent need to improve the effectiveness of systemic chemotherapy to prevent peritoneal recurrence in locally advanced GC, intraperitoneal chemotherapy (IPC) has become a valuable treatment for gastric cancer with peritoneal metastasis recently [6]. Compared with intravenous (IV) administration, IP administration can deliver chemotherapeutics with a higher concentration and a longer half-life in the peritoneal cavity, improving locoregional anti-tumor effects [8]. However, the application of IPC is hindered by several weaknesses: firstly, through simple diffusion, intraperitoneal chemotherapeutics can penetrate only 2–3 mm of peritoneal nodule [9]. Secondly, due to gravity, not all metastasis in abdominal cavity can be reached by drug solution [10]. Thirdly, fragile peritoneum and abdominal organs also suffer from chemotherapeutics diffused in abdominal cavity, causing severe complications such as peritonitis and intestinal obstruction [11]. In clinical

* Corresponding author.
** Corresponding author.
E-mail addresses: baoruiliu@nju.edu.cn (B. Liu), rutianli@nju.edu.cn (R. Li).
[1] These authors are contributed equally to this work.

application, to make all metastasis distributed in abdominal cavity in touch with drugs, patients are recommended to hold different clinostatism postures for several hours [12]. Worse yet, repeated abdominal punctures can increase the risk of infection. Therefore, only a small population can tolerate repeated IPC.

To enhance the efficacy and safety of IPC, we established the gelatinase-responsive "double phase" nanocomplex for IPC of gastric cancer with peritoneal metastasis. Considering the sensitivity of the peritoneal cavity to foreign objects [10], we chose biocompatible material polyethylene glycol (PEG)-poly (ε-caprolactone) (PCL), which has been applied in US FDA-approved formulations. The nanocomplex is composed of PEG-pep-PCL gelatinase-responsive nanoparticles and liquid PEG-PCL-PEG (PECE) thermosensitive nanohydrogel. PECE can quickly transform from injectable flowing solution at low temperature into a nonflowing gel state when injected into abdominal cavity with normal body temperature [13] (Fig. 1a). Gelatinases are highly secreted by gastric cancer cells, when NPs are fixed by the PECE gel to the tumor tissue, the mPEG-PCL conjugates will be cleaved by gelatinases, leading to improved intracellular drug concentration and reduced IPC-related side effects (Fig. 1b). Distributing homogeneously in the PECE NPs, salinomycin (SAL) and docetaxel (DOC) get access to regions of a tumor that are not in direct contact with peritoneal fluid, inhibiting cancer stem cell
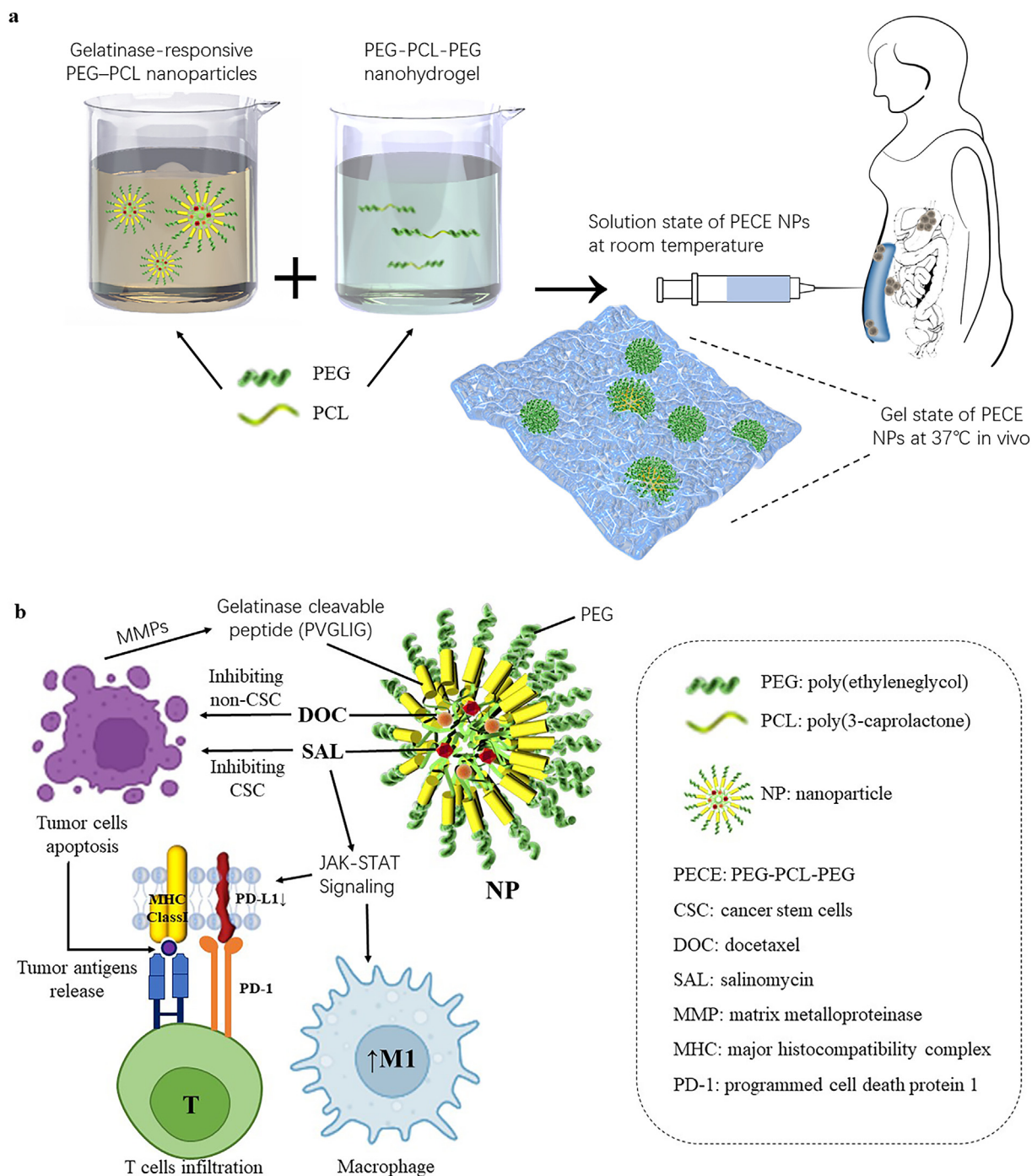

Fig. 1. Schematic diagram of intraperitoneal delivery of SAL-DOC with an in-situ crosslinkable thermosensitive nanohydrogel and gelatinase-responsive nanoparticles. (a) The scheme of PECE NPs preparation and administration. (b)Microstructure and mechanisms of SAL-DOC loaded PECE NPs.

(CSC) as well as non-CSC cancer cells all over the abdominal cavity. Moreover, the tumor treated with PECE NPs showed the lowest PD-L1 expression and the most infiltration of M1 macrophages, offsetting the immunosuppression of TME.

2. Results and discussion

2.1. Preparation of SAL-DOC nanocomplex

As we previously reported [14], SAL and DOC were initially loaded into gelatinase-responsive nanoparticles. The average diameter of NPs was 192.0 ± 0.7 nm (average and standard deviation of 4 independently prepared batches) with a zeta potential of -2.53 ± 0.33 mV (average and standard deviation of 3 independently prepared batches) at pH 7.4 (Fig. S1a). The drug loading contents of SAL and DOC were $5.54 \pm 0.06\%$ and $7.75 \pm 0.56\%$. The encapsulation efficiency of SAL and DOC were $58.75 \pm 0.61\%$ and $42.01 \pm 3.50\%$, respectively.

According to the TEM observation, the gels possessed obvious porous structure, whose distribution was uniform, resulting in good carrying capacity. The prepared SAL-DOC NPs exhibited a spherical-like shape with a smooth surface (Fig. 2a), which collapsed morphologically after incubation with gelatinase for 24 h (Fig. 2b). The result demonstrated that the NPs can be sensitively stimulated by gelatinases, which are highly secreted by gastric cancer cells specifically [15]. When applied to IPC, the nanocomplex will cause less harm to normal abdominal organs than free chemotherapeutics solution administered intraperitoneally.

2.2. In vitro cytotoxicity of NPs to cultured gastric cancer cells

Free SAL-DOC and SAL-DOC NPs (SAL and DOC co-loaded in NPs were co-cultured with MGC803 cells under equivalent concentrations for 48 h, and the percentage of the viable cells was examined. NPs showed less cytotoxicity than free SAL-DOC when the cellular exposure was limited to 12 h ($p < 0.05$), which may attribute to the sustained release effects of the nanoparticles and the absence of gelatinase targeting when drugs were added to the culture solution. In contrast, when MGC803 cells were exposed to NPs for more than 48 h, there was no difference between Free SAL-DOC and NPs in the cytotoxic activity (Fig. S1b) due to the majority of SAL and DOC would have been released from the gelatinase-responsive nanoparticles after the 2-day-cocculturation with gastric cancer cells (Fig. S2a and b), inhibiting CSC as well as non-CSC cancer cells. The sustainable release pattern will lead to long-term anti-tumor effect and much more moderate side effects.

2.3. Cytotoxicity of PECE NPs to multicellular spheroids

Multicellular tumor spheroids (MCTs) have been considered as a good way to simulate tumor tissue in vivo. Observed under light microscope, tumor spheroid was entirely wrapped by PECE NPs (Fig. S1c and d). Using laser scanning confocal microscopy, we visualized tumor cell killing to quantify cell mortalities of MCTs. Representative images indicated that the cooperation of PECE gel with NPs or free SAL-DOC significantly reduced living cells throughout the MCTs, and PECE NPs showed the best cytotoxicity (Fig. 3). This stereoscopic ex vivo study further confirmed the anti-tumor effect of PECE NPs.

2.4. The real-time biodistribution of nanoparticles

To investigate the biodistribution and metabolism of PECE NPs in vivo, we used bis (trihexylsiloxy) silicon 2,3-naph-thalocyanine to track the in vivo dynamic distribution of PECE NPs and NPs. Whole-body near infrared (NIR) imaging demonstrated that PECE NPs mainly accumulated in abdominal cavity and reserved there for more than 96 h. However,

when the NIR dye was loaded in NPs, it distributed from abdominal cavity into systemic circulation, and had shown highest concentration in lung since 12 h after intraperitoneal injection (Fig. 2d). The NIR results indicated that the PECE NPs have the ability to retain the most drugs in abdominal cavity compared with NPs.

2.5. In vivo antitumor effect

The effectiveness of IP-administered treatments was tested on animal model. Nude mice bearing MGC-803-luc tumors in the peritoneal cavity were evaluated via non-invasive in vivo imaging system. The tumor burden increased significantly in the Blank group, which was consistent with that of PBS group (Fig. 4a). Free SAL-DOC and PECE/Free SAL-DOC suppressed the tumor growth effectively, demonstrating the in-vivo antitumor effect of SAL-DOC combination when intraperitoneally administrated (Fig. 4c). However, the metastatic tumors weren't completely removed, which re-grew after an initial attenuation over 1–2 weeks (Fig. 4c). To explain, as lipid-soluble drugs, SAL and DOC can hardly distribute in the extracellular matrix (ECM) and therefore rarely diffuse around all tumor cells.

Among all the groups, NPs and PECE NPs inhibited tumor growth most remarkably, some of which even achieved CR (complete response) and continued for more than 2 weeks (Fig. 4c). Located in the oil phase of NPs, SAL and DOC are endowed with better solubility and bioavailability, increasing the drugs concentration in tumor sites. Carried in the nanocomplex, the nanoparticles release drugs in a more sustained fashion, prolonging the local effect and attenuating systemic drug absorption. Regrettably, because of the excellent therapeutic effect of mere NPs, the advantage of PECE NPs was not statistically significant.

2.6. In vivo toxicity study

Salinomycin is known for its severe side effects such as neural and respiratory system toxicity [16], so it has not been approved for clinical use. In our previous study [17], we found that all BALB/c nude mice survived after IP injection of SAL NPs at the dose exceeding the lethal dose of SAL, which demonstrated gelatinase-responsive nanoparticles can reduce the side effects of Salinomycin. In this study, to improve the effectiveness and tumor targeting ability of the system, the hydrogel was administrated along with gelatinase-responsive nanoparticles, which specifically recognize matrix metalloproteinase (MMPs) that were highly expressed into tumor microenvironment (TME) [18] by gastric cancer cells. Once carried by PECE NPs, SAL would reach the interstitium of tumor tissues from leaky tumor blood vessels and be held within the tumor because of the pressure made by destitute lymphatic drainage, causing less damage to normal organs. The body weight of mice treated with free SAL-DOC decreased significantly ($p < 0.01$), while PECE NP and NP group did not show changes in their body weight (Fig. 4b). We did H&E-stained sections of all important organs. In free SAL-DOC group, the small intestinal villi were distorted and shortened, while PECE NPs group didn't show any chronic injuries (Fig. S3a). As for lung tissue, the degree for infiltration of inflammatory cells, alveolar hyperemia and hydrops from the severe to the mild were free SAL-DOC, PECE/Free SAL-DOC, NP and PECE NP(Fig. S3a). The differences of weight and pathological changes between PECE NP group and free SAL-DOC group were compelling evidence for the safety of our nanocomplex.

2.7. PECE NPs inhibit the stem-like tumor cells in vivo

Cancer stem cells (CSCs) play an important role during the occurrence and development of the upper gastrointestinal cancer [19]. Endowed with stem-like features as well as potential to sustain tumorigenesis constantly, CSCs drive cancer growth and reconstruct their heterogeneity
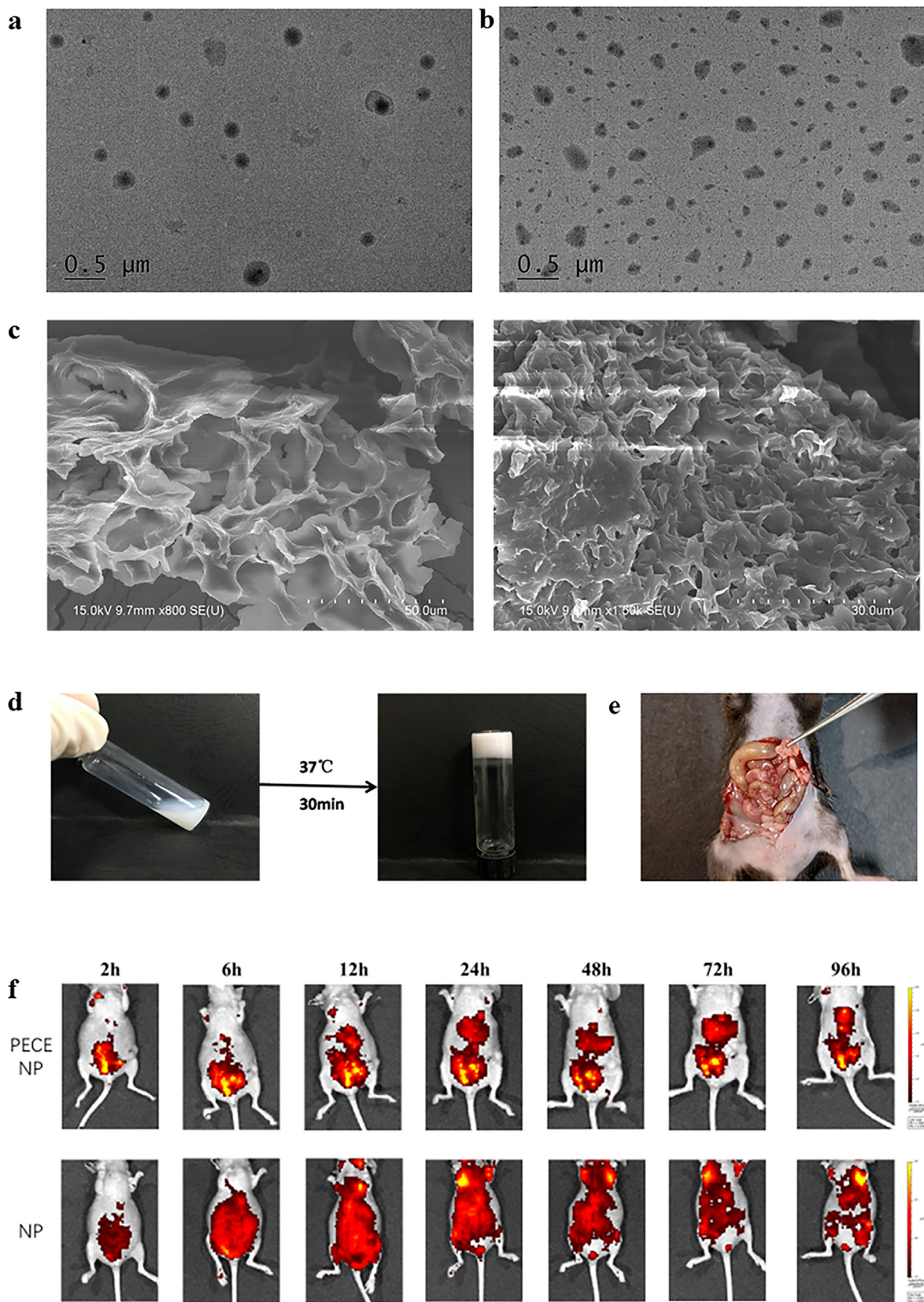
Fig. 2. The TEM images of SAL-DOC NPs before (a) and after (b) incubation with Collagenase IV. (c)The TEM images of PECE nanohydrogel (d)Thermosensitive behavior of the PECE NPs at 10 °C and 37 °C. (e)Thermosensitive behavior of the PECE NPs in vivo. (f) The real-time biodistribution of NIR-775 loaded PECE NPs and NPs.
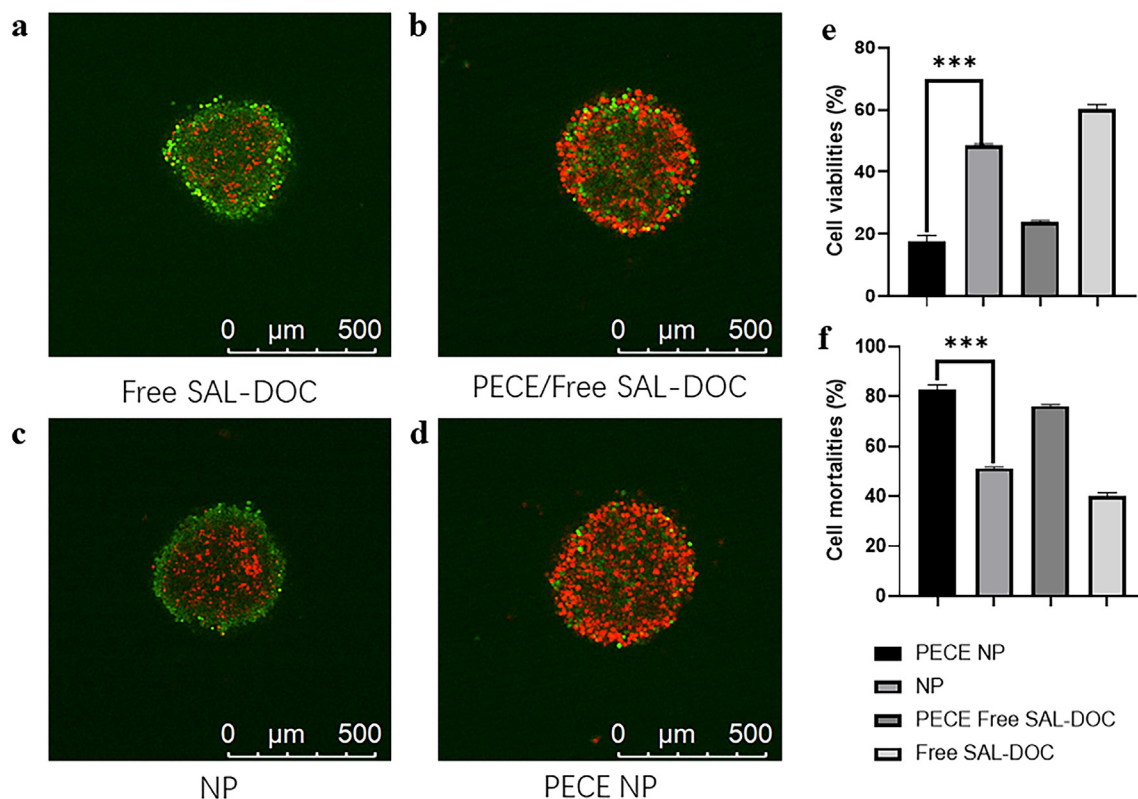
Fig. 3. Cytotoxicity of PECE NPs to multicellular spheroids. Representative confocal images of MGC803 spheroids treated with Free SAL-DOC(a), PECE/Free SAL-DOC(b), NP(c) and PECE NP(d). Dead cells: Propidium Iodide (red); live cells: calcein AM (green). Cell viabilities(e) and cell mortalities(f) of MGC803 spheroids. Scale bar, 500 μm. Data represent mean ± s.e.m., n = 3.

[20]. Density of CSCs in tumor tissues is reflected by the evaluation of the rate of expressions for related genes and protein signature, among which CD44 and CD133 are used to identify CSCs in gastrointestinal cancer [21]. According to the cytometric analysis of cellular suspension from abdominal tumor tissues, the proportion of CSCs (CD44+CD133+) in the free SAL-DOC group was lower than that of control group. Treated with NPs, the proportion of CSCs was much lower, and that of PECE NP group was the lowest (Fig. 5a). As a CSC inhibitor, SAL specifically eradicates CSCs by attenuating the EMT pathway, accordingly suppressing tumor growth and recurrence. However, the applications of SAL are limited due to its severe side effects and poor aqueous solubility. Through enhanced permeability and passive targeting effect, SAL can enter and remain in the tumor sites when loaded in NPs and carried by PECE gel, improving the safety and tolerability of drugs. Biodegradable nanohydrogel has been wildly investigated as a delivery vector to load chemotherapeutic drugs for intraperitoneal infusion chemotherapy, among which PECE hydrogel is known for its softness and stabilization at body temperature, hardly doing harm to abdominal organs. When applied along with NPs to deliver CSC inhibitor, PECE gel can add more extra contact access to the peritoneal metastasis, suppressing CSCs more favorably.

2.8. PECE NPs induced local antitumor inflammations

In the past few years, the remarkable results have put immunotherapy under the spotlight, among which the PD-L1/PD-1 pathway stood out due to its proven value as a therapeutic target in various malignancies [22]. Through binding to its receptor PD-1 on activated T cells, PD-L1 inhibits anti-tumor immunity by counteracting T cell-activating signals. In this study, the tumor cells treated with PECE NPs showed the lowest

PD-L1 expression (Fig. 5b), offsetting the immunosuppression of TME. The 3D structure of the hydrogel has been considered to resemble the lymph nodes, which is endowed with loading capacity for T cells reproduction [23]. Combined with the loading NPs here, the nano-complex result in an increased T cells and macrophages infiltration (Fig. 6a). Our results prompted that intraperitoneally administrated hydrogel can be an effective and feasible approach for inflaming these so-called immune desert tumors.

Salinomycin has been demonstrated to repolarize tumor-associated macrophage (TAM) toward the TAM-1 phenotype through STAT1/STAT3 regulation [24]. Recently, more and more evidence shows that CSCs facilitate tumor progression through transforming TME via distinct mechanisms, such as increased infiltration of macrophages and microglia [25]. In this study, we found that tumors treated with PECE NPs were infiltrated with more TAM-1 (CD11b+F480+CD86+), which participate in antigen presentation and play an anti-tumorigenic role (Fig. 6b). Owing to targeting delivery of PECE NPs, SAL was delivered to the tumor site more efficiently and specifically, promoting the infiltration of TAM-1. According to the viewpoint of Bruni et al. [26], the expression of PD-L1 as well as infiltration of TAM-1 are both important positive prognosis of gastric cancer. Therefore, PECE NPs not only suppressed CSC and non-CSC tumor cells directly, but also induced local antitumor inflammations to inhibit gastric cancer progression.

3. Conclusion

In summary, this study represents an example of gelatinase-responsive NPs combined with thermosensitive hydrogel, both of which were prepared from PECE with different compositions, for IPC of
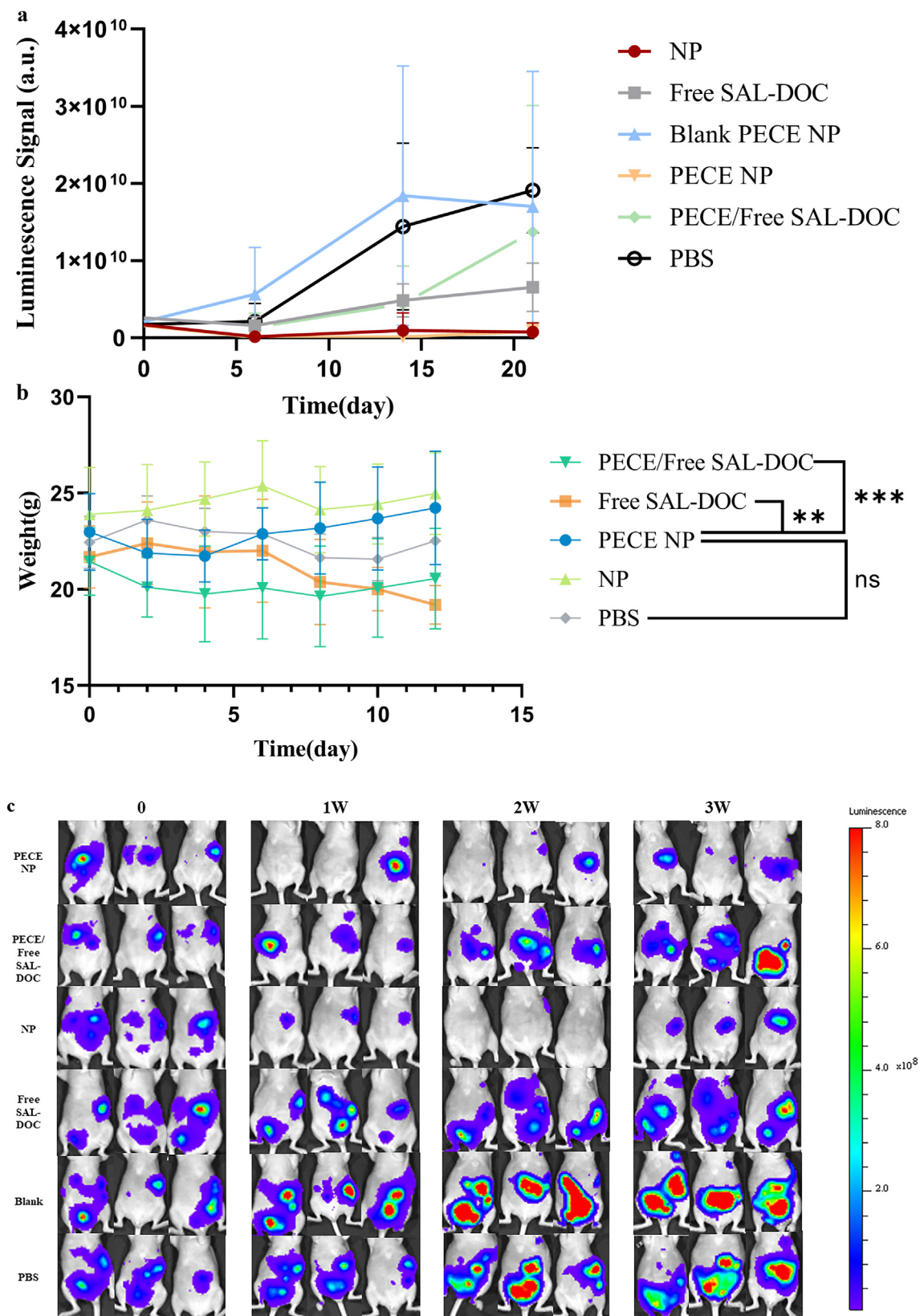
Fig. 4. (a)Bioluminescence of IP tumors in animals treated with PECE NP, NP, PECE/Free SAL-DOC, Free SAL-DOC, BLANK PECE NP, PBS. (b) Weight loss profiles over time after various treatments. (c) Whole body bioluminescence imaging of animals administered with different treatments.
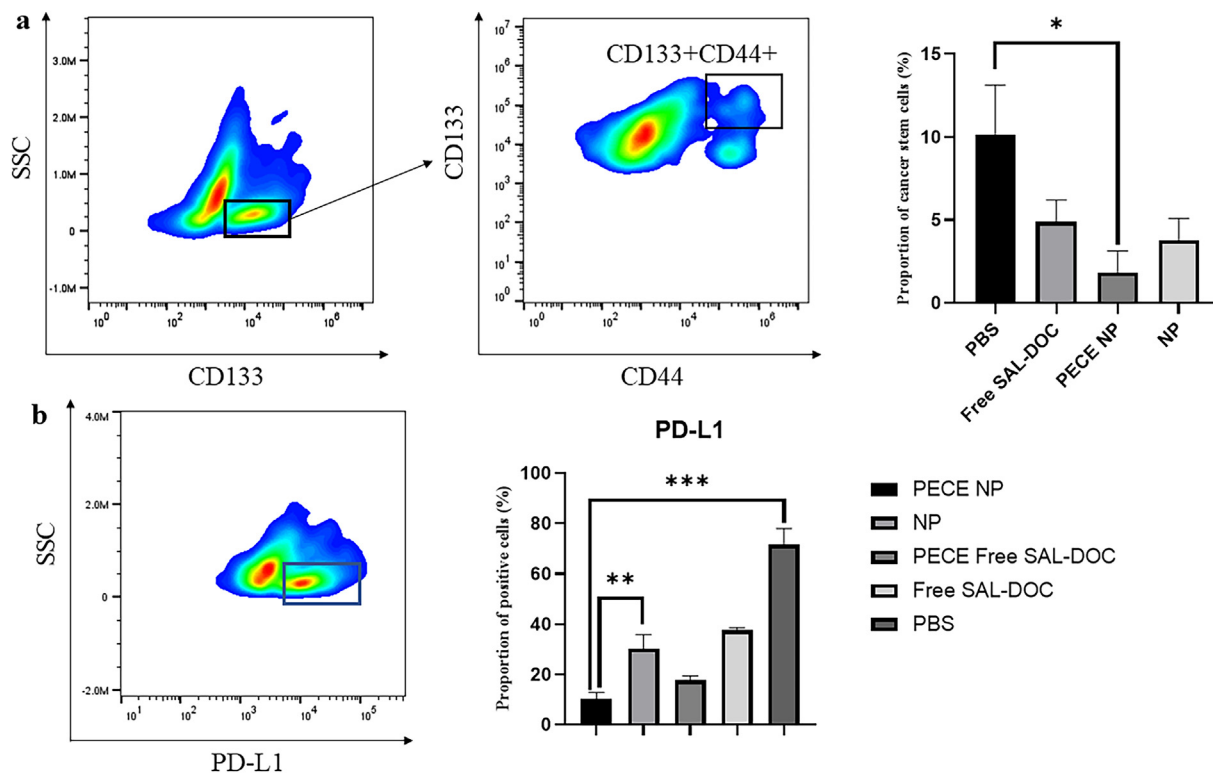
Fig. 5. Flow cytometric analysis of single cell suspensions from xenograft abdominal tumor tissues. (a)Quantifying proportion of cancer stem cells (CD133+CD44$^+$) of human gastric cancer cells (b)Quantifying expression of PD-L1 on human gastric cancer cell surface.

gastric cancer therapy. PECE NPs not only showed a greater antitumor efficacy than SAL-DOC solution administered at the same dose, but also mitigate side effects of SAL-DOC caused to normal abdominal organs and peritoneum. This compound nano-drug system shows great superiority in simultaneously delivering the two payloads into the same tumor cell disseminated in the abdominal cavity, especially decreased CD44 expression to suppress CSCs, thus PECE NPs can remarkably inhibit tumor growth in a synergistic manner. At the same time, tumors treated with PECE NPs showed the lowest PD-L1 expression and most TAM-1 infiltration, demonstrating the potential of nanocomplex to inflame immune desert tumors.

4. Materials and methods

4.1. Materials

Polyethyleneglycol-NHS (PEG-NHS) was synthesized by Beijing Jiankai Technology Company (Beijing, China). The gelatinases-cleavable peptide (PVGLIG) was synthesized by Shanghai HD Biosciences Company (Shanghai, China). Cell culture medium and supplements were purchased from Gibco (NY, USA). All other reagents including Salinomycin and Docetaxel were purchased from Macklin (Shanghai, China). Mouse CD3 and CD68 antibodies were purchased from Servicebio (Wuhan, China). Human CD44 and CD133 antibodies were purchased from Bio-Legend (CA, USA).

4.2. Preparation and characterization of gelatinase-responsive nanoparticles

PEG-pep-PCL copolymers were prepared as we previously described [14]. Nanoparticles were prepared using a double-emulsion method. Briefly, SAL and DOC were dissolved in DCM at 10 mg/mL, and then added to PEG-pep-PCL dichloromethane solution. The mixture was

homogenized with 5% w/v PVA solution using probe sonication (XL2000, Misonix, USA) at 27.5 W for 60 s. This water/oil (w/o) emulsion was transferred to an aqueous solution 1% w/v PVA, and the mixture was probe-sonicated at 17.5 W for 30 s. The resulting w/o/w emulsion was then mechanically stirred for 2 h to remove DCM. The NPs were purified by centrifugation at 15,000 rpm for 30 min (Leiboer LG16B centrifuge, Beijing, China) and reconstituted two times with deionized and distilled water.

4.3. Preparation of in-situ crosslinkable PECE nanohydrogel loaded with NPs

PEG–PCL diblock copolymers were synthesized through ring-opening polymerization of ε-CL initiated by MPEG. PEG–PCL diblock copolymers were coupled with the coupling agent HMDI, the PEG–PCL–PEG triblock copolymers were eventually obtained [27].

Aqueous PECE solutions were prepared by dissolving PECE copolymers in deionized water at a designated temperature then cooled to 4 °C. PECE solutions were mixed with the pre-cooling NPs or free SAL-DOC solution under mild agitation to obtain homogeneous liquid solution.

4.4. Cytotoxicity of SAL-DOC NPs

MGC803 human gastric cancer cells (ATCC) were seeded into a 96-well plate at a concentration of 5000 cells every well. After 24 h, NP or free SAL-DOC solution was added to each well to provide DOC of 10 μg/mL and SAL of 7 μg/ml in the final concentration. The cell viability was estimated by the Cell-Counting Kit 8 (CCK8) assay. Fluorescence (450 nm) was recorded in a microplate reader.

Multicellular tumor spheroids were formed from MGC803 cultured in 96 Well Clear Round Bottom Ultra Low Attachment Microplate (Corning, USA). When the spheroids grew to 200 μm in diameter, PECE NPs, NPs,
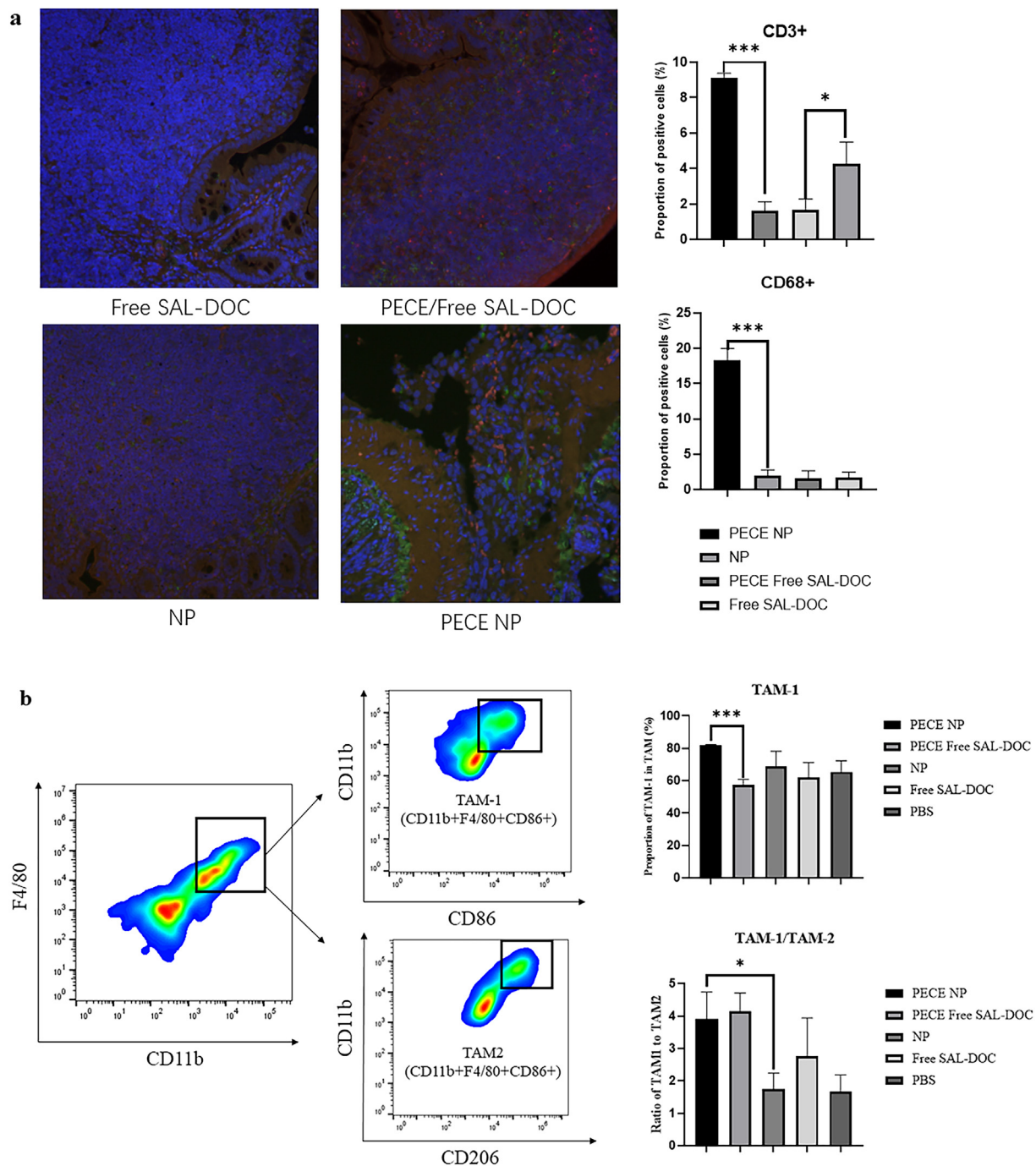
Fig. 6. Immunoassay of allograft abdominal tumor tissues (a) Multispectral immunofluorescence imaging reveals T cells (CD3^{+}, red) and macrophages (CD68^{+}, green) infiltration in tumors after 8 days of treatment (200× magnification, DAPI nuclear counterstaining). (b) Quantifying proportion of TAM-1 and TAM-2 in single cell suspensions from allograft abdominal tumor tissues by flow cytometry.

PECE/Free SAL-DOC and Free SAL-DOC were added, and final concentrations were DOC of 10 μg/mL and SAL of 7 μg/ml in all groups. After incubation for 12 h at 37 °C, the spheroids were washed, stained using a Viability/Cytotoxicity Kit (Beyotime, China). Confocal microscope (Leica, Germany) was used as Z-stack projects scanning from the top to the middle of the MCTs with 10 μm intervals and then presented as maximum intensity projections. To quantify live/dead cells, the total cell area of each dye was measured with ImageJ.

4.5. Real-time near-infrared fluorescence imaging

Bis(trihexylsiloxy)silicon 2,3-naph-thalocyanine (Sigma, Germany) was labeled in PECE NPs and NPs according to the method described in 4.2 and 4.3. Then unconjugated dye was removed by dialysis (MWCO 3500 Da) for 2 days. Labeled NPs and PECE NPs were injected intraperitoneally to Balb/c nude mouse. At different time intervals, the mice were anesthetized and scanned using an IVIS Lumina III system (PerkinElmer, Massachusetts, USA).

4.6. Anti-tumor efficacy of treatments in an IP tumor model

Luciferase-expressing MGC803 cells (MGC803-luc) were cultured in a complete RPMI-1640 medium. Two million cells were suspended in 0.3 mL PBS and intraperitoneally injected to a Balb/c nude mouse (female, 5–6 weeks old, ~20 g, Model Animal Research Center of Nanjing University). Two weeks later, mice with different tumor burdens were evenly assigned to six groups (n = 6 per group) and intraperitoneally administered with PBS, Blank PECE NP, free SAL-DOC, PECE/free SAL-DOC, NPs, and PECE NPs (at the dose of DOC 3 mg/kg and SAL 2.2 mg/kg). Bioluminescence of IP tumors was measured weekly using the IVIS Lumina III system (PerkinElmer, Massachusetts, USA).

4.7. Immune effects of treatments in an IP tumor model

Mouse forestomach carcinoma (MFC) cells were cultured in complete RPMI-1640 medium. 3×10^5 cells were suspended in 0.3 mL PBS and injected to a female 615 mouse (female, 5–6 weeks old, Nanjing Junke Biotechnology). One week later, mice were evenly assigned to six groups (n = 4 per group) and administered with PBS, Blank PECE NP, free SAL-DOC, PECE/free SAL-DOC, NPs, and PECE NPs (at the dose of DOC 3 mg/kg and SAL 2.2 mg/kg). One week after the treatment, all mice were sacrificed to collect tumor samples for immune analysis.

4.8. Production of single cell suspensions from abdominal tumor tissues

Mice were euthanized to harvest the peritoneal metastasis tumors. The tumors were placed on the 70 μm strainer (BD Biosciences). Wet by cold media, the tumors were gently ground and single cell suspensions would pass through strainers. To collect all the splenocytes, the strainer was then washed using cold media. After centrifugation and resuspension, the suspension was finally obtained.

4.9. Study on the types of immunocytes infiltrated in tumor by flow cytometry

The cells were then stained with tetramer in FACS buffer in the dark at room temperature for half an hour and then washed twice. Single staining was done for each of the antibodies for appropriate flow cytometry compensation. The type of immunocytes and tumor cells were analyzed with FlowJo software.

4.10. Multispectral immunofluorescent imaging

Fixed in 4% neutral buffered formalin for at least 24 h, tumor samples were processed for dehydratation and paraffinization. After antigen-repairing, slides were managed for deparaffinization, epitope retrieval and endogenous peroxidase quenching. The multiplex staining method included several rounds of staining [28]. In every round, blocking the non-specific site, slides were incubated with unlabeled primary antibody and then the HRP-conjugated secondary antibody (GB23303, Servicebio). Nuclear staining was performed using Spectral DAPI dye solution (G1012, Servicebio). Multiplex IF images from the stained slides were acquired through Pannoramic MIDI: 3Dhistech multispectral microscope.

4.11. Statistical analysis

The Student's t-test (two-tailed) was used for statistical analyses. P-value style: *p < 0.05; **p < 0.01; ***p < 0.005. All statistical analyses were performed using SPSS Statistics 26 software. Graphs were created using GraphPad Prism version 8.00 unless otherwise stated.

Author contributions

Xinyue Wang, Baorui Liu and Rutian Li designed the experiments and interpreted the results. Xinyue Wang, Jiahui Gao and Chunhua Li performed experiments. Chen Xu and Xiang Li assisted with the experimental work. Xinyue Wang wrote the manuscript, prepared figures and performed the statistical analysis. Qin Liu, Qin Wang and Lixia Yu assisted in manuscript preparation. Fanyan Meng, Baorui Liu and Rutian Li supervised the study and verified the results. All authors read and approved the final manuscript.

Declaration of competing interest

The authors declare that they have no known competing financial interests or personal relationships that could have appeared to influence the work reported in this paper.

Acknowledgments

Appendix A. Supplementary data

Supplementary data to this article can be found online at https://doi.org/10.1016/j.mtbio.2022.100305.

References

[1] S.S. Joshi, B.D. Badgwell, Current treatment and recent progress in gastric cancer, CA A Cancer J. Clin. 71 (3) (2021) 264–279.

[2] R. Sitarz, M. Skierucha, J. Mielko, G.J.A. Offerhaus, R. Maciejewski, W.P. Polkowski, Gastric cancer: epidemiology, prevention, classification, and treatment, Cancer Manag. Res. 10 (2018) 239–248.

[3] I. Thomassen, Y.R. van Gestel, B. van Ramshorst, M.D. Luyer, K. Bosscha, S.W. Nienhuijs, V.E. Lemmens, I.H. de Hingh, Peritoneal carcinomatosis of gastric origin: a population-based study on incidence, survival and risk factors, Int. J. Cancer 134 (3) (2014) 622–628.

[4] A.P. Thrift, H.B. El-Serag, Burden of gastric cancer, Clin. Gastroenterol. Hepatol. 18 (3) (2020) 534–542.

[5] R.A. Seshadri, O. Glehen, Cytoreductive surgery and hyperthermic intraperitoneal chemotherapy in gastric cancer, World J. Gastroenterol. 22 (3) (2016) 1114–1130.

[6] P.E. Bonnot, G. Piessen, V. Kepenekian, E. Decullier, M. Pocard, B. Meunier, J.M. Bereder, K. Abboud, F. Marchal, F. Quenet, D. Goere, S. Msika, C. Arvieux, N. Pirro, R. Wernert, P. Rat, J. Gagniere, J.H. Lefevre, T. Courvoisier, R. Kianmanesh, D. Vaudoyer, M. Rivoire, P. Meeus, G. Passot, O. Glehen, Fregat, B.-R. Networks, Cytoreductive surgery with or without hyperthermic intraperitoneal chemotherapy for gastric cancer with peritoneal metastases (CYTO-CHIP study): a propensity score analysis, J. Clin. Oncol. 37 (23) (2019) 2028–2040.

[7] J. Kitayama, H. Ishigami, H. Yamaguchi, Y. Sakuma, H. Horie, Y. Hosoya, A.K. Lefor, N. Sata, Treatment of patients with peritoneal metastases from gastric cancer, Ann. Gastroenterol. Surg. 2 (2) (2018) 116–123.

[8] B.L. Brucher, P. Piso, V. Verwaal, J. Esquivel, M. Derraco, Y. Yonemura, S. Gonzalez-Moreno, J. Pelz, A. Konigsrainer, M. Strohlein, E.A. Levine, D. Morris, D. Bartlett, O. Glehen, A. Garofalo, A. Nissan, Peritoneal carcinomatosis: cytoreductive surgery and HIPEC–overview and basics, Cancer Invest. 30 (3) (2012) 209–224.

[9] A.C. Gamboa, J.H. Winer, Cytoreductive surgery and hyperthermic intraperitoneal chemotherapy for gastric cancer, Cancers 11 (11) (2019).

[10] E.J. Cho, B. Sun, K.O. Doh, E.M. Wilson, S. Torregrosa-Allen, B.D. Elzey, Y. Yeo, Intraperitoneal delivery of platinum with in-situ crosslinkable hyaluronic acid gel for local therapy of ovarian cancer, Biomaterials 37 (2015) 312–319.

[11] W.J. Koemans, R.T. van der Kaaij, E.C.E. Wassenaar, C. Grootscholten, H. Boot, D. Boerma, M. Los, O. Imhof, J.H.M. Schellens, H. Rosing, A.D.R. Huitema, J.W. van Sandick, Systemic exposure of oxaliplatin and docetaxel in gastric cancer patients with peritonitis carcinomatosis treated with intraperitoneal hyperthermic chemotherapy, Eur. J. Surg. Oncol. 47 (2) (2021) 486–489.

[12] M. Orditura, G. Galizia, V. Sforza, V. Gambardella, A. Fabozzi, M.M. Laterza, F. Andreozzi, J. Ventriglia, B. Savastano, A. Mabilia, E. Lieto, F. Ciardiello, F. De Vita, Treatment of gastric cancer, World J. Gastroenterol. 20 (7) (2014) 1635–1649.

[13] M. Norouzi, B. Nazari, D.W. Miller, Injectable hydrogel-based drug delivery systems for local cancer therapy, Drug Discov. Today 21 (11) (2016) 1835–1849.

[14] Q. Wang, Y.T. Yen, C. Xie, F. Liu, Q. Liu, J. Wei, L. Yu, L. Wang, F. Meng, R. Li, B. Liu, Combined delivery of salinomycin and docetaxel by dual-targeting gelatinase nanoparticles effectively inhibits cervical cancer cells and cancer stem cells, Drug Deliv. 28 (1) (2021) 510–519.

[15] C.F. Sier, F.J. Kubben, S. Ganesh, M.M. Heerding, G. Griffioen, R. Hanemaaijer, J.H. van Krieken, C.B. Lamers, H.W. Verspaget, Tissue levels of matrix metalloproteinases MMP-2 and MMP-9 are related to the overall survival of patients with gastric carcinoma, Br. J. Cancer 74 (3) (1996) 413–417.

[16] W. Boehmerle, M. Endres, Salinomycin induces calpain and cytochrome c-mediated neuronal cell death, Cell Death Dis. 2 (2011) e168.

[17] Q. Wang, F. Liu, L. Wang, C. Xie, P. Wu, S. Du, S. Zhou, Z. Sun, Q. Liu, L. Yu, B. Liu, R. Li, Enhanced and prolonged antitumor effect of salinomycin-loaded gelatinase-responsive nanoparticles via targeted drug delivery and inhibition of cervical cancer stem cells, Int. J. Nanomed. 15 (2020) 1283–1295.

[18] A. Alaseem, K. Alhazzani, P. Dondapati, S. Alobid, A. Bishayee, A. Rathinavelu, Matrix Metalloproteinases: a challenging paradigm of cancer management, Semin. Cancer Biol. 56 (2019) 100–115.

[19] Y. Hayakawa, H. Nakagawa, A.K. Rustgi, J. Que, T.C. Wang, Stem cells and origins of cancer in the upper gastrointestinal tract, Cell Stem Cell 28 (8) (2021) 1343–1361.

[20] M. Najafi, B. Farhood, K. Mortezaee, Cancer stem cells (CSCs) in cancer progression and therapy, J. Cell. Physiol. 234 (6) (2019) 8381–8395.

[21] H. Chen, J. Lin, Y. Shan, L. Zhengmao, The promotion of nanoparticle delivery to two populations of gastric cancer stem cells by CD133 and CD44 antibodies, Biomed. Pharmacother. 115 (2019) 108857.

[22] C. Sun, R. Mezzadra, T.N. Schumacher, Regulation and function of the PD-L1 checkpoint, Immunity 48 (3) (2018) 434–452.

[23] E. Perez Del Rio, F. Santos, X. Rodriguez Rodriguez, M. Martinez-Miguel, R. Roca-Pinilla, A. Aris, E. Garcia-Fruitos, J. Veciana, J.P. Spatz, I. Ratera, J. Guasch, CCL21-loaded 3D hydrogels for T cell expansion and differentiation, Biomaterials 259 (2020) 120313.

[24] H. Shen, C.C. Sun, L. Kang, X. Tan, P. Shi, L. Wang, E. Liu, J. Gong, Low-dose salinomycin inhibits breast cancer metastasis by repolarizing tumor hijacked macrophages toward the M1 phenotype, Eur. J. Pharmaceut. Sci. 157 (2021) 105629.

[25] J.A. Clara, C. Monge, Y. Yang, N. Takebe, Targeting signalling pathways and the immune microenvironment of cancer stem cells - a clinical update, Nat. Rev. Clin. Oncol. 17 (4) (2020) 204–232.

[26] J. Galon, D. Bruni, Tumor immunology and tumor evolution: intertwined histories, Immunity 52 (1) (2020) 55–81.

[27] C. Gong, S. Shi, P. Dong, B. Kan, M. Gou, X. Wang, X. Li, F. Luo, X. Zhao, Y. Wei, Z. Qian, Synthesis and characterization of PEG-PCL-PEG thermosensitive hydrogel, Int. J. Pharm. 365 (1–2) (2009) 89–99.

[28] F.G. Herrera, C. Ronet, M. Ochoa de Olza, D. Barras, I. Crespo, M. Andreatta, J. Corria-Osorio, A. Spill, F. Benedetti, R. Genolet, A. Orcurto, M. Imbimbo, E. Ghisoni, B. Navarro Rodrigo, D.R. Berthold, A. Sarivalasis, K. Zaman, R. Duran, C. Dromain, J. Prior, N. Schaefer, J. Bourhis, G. Dimopoulou, Z. Tsourti, M. Messemaker, T. Smith, S.E. Warren, P. Foukas, S. Rusakiewicz, M.J. Pittet, S. Zimmermann, C. Sempoux, U. Dafni, A. Harari, L.E. Kandalaft, S.J. Carmona, D. Dangaj Laniti, M. Irving, G. Coukos, Low dose radiotherapy reverses tumor immune desertification and resistance to immunotherapy, Cancer Discov. 12 (1) (2021) 108–133.